The International Archives of the Photogrammetry, Remote Sensing and Spatial Information Sciences, Volume XLVIII-1/W2-2023
ISPRS Geospatial Week 2023, 2–7 September 2023, Cairo, Egypt

GIS INTEGRATION OF LAND COVER WITH NIGHT-TIME LIGHTS FOR SPATIOTEMPORAL EVALUATION OF URBAN EXPANSION

Srashti Singh[*,1], Kamal Jain[1], Anugya Shukla[2]

[1]Geomatics Group, Department of Civil Engineering, Indian Institute of Technology Roorkee, India
[2] Jamsetji Tata School of Disaster Studies, Tata Institute of Social Sciences, Mumbai, India.
[*,1]srashtisingh2018@gmail.com, [1]kjainfce@iitr.ac.in, [2]anugya.shukla@tiss.edu

KEYWORDS: Night-time lights, Urban expansion, Built-up density, GIS, Remote sensing.

ABSTRACT:

Monitoring the urbanisation process requires accurate knowledge of the present and historical spatial extents of built-up area. Understanding the quantification of urban growth is a crucial component of urban and environmental planning. The current research is focussed on evaluating the spatiotemporal change evaluation of built-up area by using a combination Landsat 8 and NPP-VIIRS datasets with GIS integration. Firstly, spatial change analysis of the built-up area was done by employing the Land Use and Land Cover (LULC) classification methodology for the years 2014 and 2022. This was done using the Random Forest (RF) classifier within the Google Earth Engine (GEE) platform. Secondly, the change in built-up area was evaluated with respect to the NTL data. The night-time light (NTL) images detect artificial lights being radiated from cities at night. The NTL data was categorised into three classes and later used to categorise the built-up area into ‘core urban’, ‘peri-urban’ and ‘rural’. The proportion of 'core urban' pixels experienced substantial growth, increasing from 9.8% to 15.5% of the total pixels between 2014 and 2022. This represents a notable increase of 58.75%. Conversely, the 'peri-urban' pixels saw a smaller increase of 4.6%, while the 'rural' pixels witnessed a decline of 8.7%. The average built-up density of the 'core urban' area exhibited an increase from 0.385 in 2014 to 0.398 in 2022. These changes can be attributed to the progressive conversion of 'rural' pixels into 'peri-urban' areas, and subsequently, the transformation of 'peri-urban' areas into 'core urban' regions.

1. INTRODUCTION

Urbanisation is a complex dynamic that involves growing populations, intensified socioeconomic activity, and spatially increased built-up areas and infrastructures (Cohen, 2006). Understanding the environmental effects of anthropogenic resource consumption and landscape change in the context of environment and resource sustainability requires proper measurement of the spatiotemporal aspects of urban development (Weng, 2012). Monitoring the urbanisation process requires accurate knowledge of the present and historical spatial extents of built-up urban area. Understanding the quantification of urban growth is a crucial component of urban and environmental planning, analysing the driving forces of urban development, and policy making (Rehman, Honap, Siddiqui, Maske, & Maithani, 2021; Seto & Fragkias, 2005). By utilizing remote sensing data, researchers can observe and track changes over time, allowing for a comprehensive understanding of the evolving landscape. The high spatial and temporal resolution of remote sensing imagery enables the detection and quantification of subtle or rapid changes that may not be easily discernible through traditional ground-based methods (Shukla, Jain, Ramsankaran, & Rajasekaran, 2021). Remotely sensed data has proved to have advanced capabilities to be extensively used for the delineation of the urban land (Massetti, 2020). In a changing world, long-term archives of satellite-based measurements of anthropogenic night time brightness offer an effective tool to continually track current human activity and socioeconomic dynamics during urban processes (Ma et al., 2015). A notable characteristic of nightlight data is that remotely sensed changes in anthropogenic night time lighting signals can be quantitatively linked to concurrent changes in demographics, the economy, energy consumption, and urban extent. This is in contrast to other satellite products, which primarily focus on mapping land cover (He, Zhang, & Yang, 2021). The night-time light (NTL) images detect artificial lights being radiated from cities due to human activities at night.

Researchers from across the world frequently utilise NTL data to estimate urban sprawl and map out human population distribution (Liu et al., 2022; Zhang & Seto, 2013). The Operational Linescan System (OLS) onboard the US Defence Meteorological Satellite Programme (DMSP), in use since the early 1970s, is the most frequently utilised sensor (Yücer & Erener, 2018). Numerous studies have been published that use DMSP-OLS images to show how it may be used in the social sciences as a substitute for demographic data, economic activity, greenhouse gas emissions, light pollution, disaster preparedness, urban dynamics, and epidemiology (Levin & Duke, 2012). The National Oceanic and Atmospheric Administration (NOAA)/National Geophysical Data Centre (NGDC) launched the Suomi National Polar-Orbiting Partnership (NPP) satellite with the Visible Infrared Imaging Radiometer Suite (VIIRS) in October 2011. In comparison to DMSP/OLS, NPP-VIIRS NTL data are the new generation of NTL data and have improved spatial and radiometric resolution (15 arc seconds, 0.5 km 0.5 km), radiometric detection range, and onboard calibration (Wang, Fan, & Wang, 2019). The NPP-VIIRS data have been adapted to be a good indication of human activities, land use, and economy based on the aforementioned superiorities (Li, Li, Xu, & Wu, 2017).

Numerous studies have provided novel insights in distinguishing urban boundaries using NPP-VIIRS data (Kabanda, 2022). Despite the fact that NTL data might offer additional details, researchers nevertheless came to the conclusion that the lack of residential data limits the increase of estimation accuracy. As a result, past investigations were used to acquire land observation data (Wang et al., 2019). To analyse the urban growth in Kimberley, South Africa, Kabanda (Kabanda, 2022) used remote sensing data (Landsat satellite data) to quantify urban expansion from 2013 to 2018. Data from night time lights can offer important insights regarding the population density of an urban area.

*Corresponding author

Even while information about night time lights doesn't directly quantify the size of buildings, it can be used to infer urban development and human activity. Night-time lights data can be calibrated and validated using ground-truth data, such as building inventories, census information, or high-resolution imagery. The association between night time illumination and urban areas is predicated on the idea that places with higher night time brightness typically correspond to regions with greater urbanisation and built infrastructure. The intensity of social and economic activity, patterns of urbanisation, population density, and the presence of buildings and infrastructure can all be reflected in the brightness and density of lights. Examining trends in night time light data over the course of time can reveal information on urban development and the rise of built-up areas.

The current research is focussed on the spatiotemporal change evaluation of urban densities of differently developed areas of an Indian city by using a combination of multi-source and multi-temporal datasets with GIS integration. The change analysis is carried out by comparing the night time data with the land cover classified data for different urban regions of the city. Lastly, it is concluded how land cover classification is a good measure when used in addition to night time data. The policymakers and municipal authorities can utilise such a study to map and manage future development in the city and make it more controlled, smart, and sustainable.

2. STUDY AREA

The area investigated for the current study is the Bhopal city located in the Madhya Pradesh state of India as depicted in Figure 1. It is densely populated as it is the state capital of Madhya Pradesh. It lies between longitudes 77°12' and 77°40' east and latitudes 23°07' and 23°54' north. At an average altitude of 1400 feet, Bhopal experiences an average annual rainfall of 1140 mm. From mid-March to early June, before the monsoon, it is very hot, and from mid-November to late February, nights are very cold.

Bhopal, the twentieth-largest urban agglomeration in the world and the sixteenth-largest city in India, is also one of the twenty-one cities with the greatest growth rates worldwide (Singh & Jain, 2022). Due to the capital city's steady and unceasing development, its population is growing rapidly, and the city boundary is expanding tremendously. The Master Plan 2030 for the city considers a planning area which is bigger than the Bhopal Municipal Corporation (BMC) area (Government of MP, 2020). In this research, our study was centred on the planning area of Bhopal, encompassing a vast expanse of 814 km^2. This choice of area was deliberate. It is twice the size of the BMC (Bhopal Municipal Corporation) area, which spans 418 km^2. By considering this larger planning area, we aimed to capture a more comprehensive and representative sample of the regions with different urban development patterns. This expanded scope provides valuable insights into the spatial and temporal aspects of Bhopal's growth and development.

3. DATASETS USED

The map of Bhopal planning area boundary and water bodies was obtained from the Bhopal Municipal Corporation office. The projection for both the datasets used is uniformly set to Geographic Coordinate System, WGS84, UTM Zone 43N. Table 1 provides the specifications of the datasets used.

Urban Sprawl: For getting the land use land cover (LULC) data and subsequently extracting the urbanised areas, Landsat 8 Level 2 (atmospherically adjusted ready-to-use data), Collection 2 (increased data quality compared to collection 1), Tier 1 (highest radiometric and positional quality), surface Reflectance data are utilised. The images used were for February because the lack of lush foliage in this month makes it simpler to distinguish between different land cover classes.

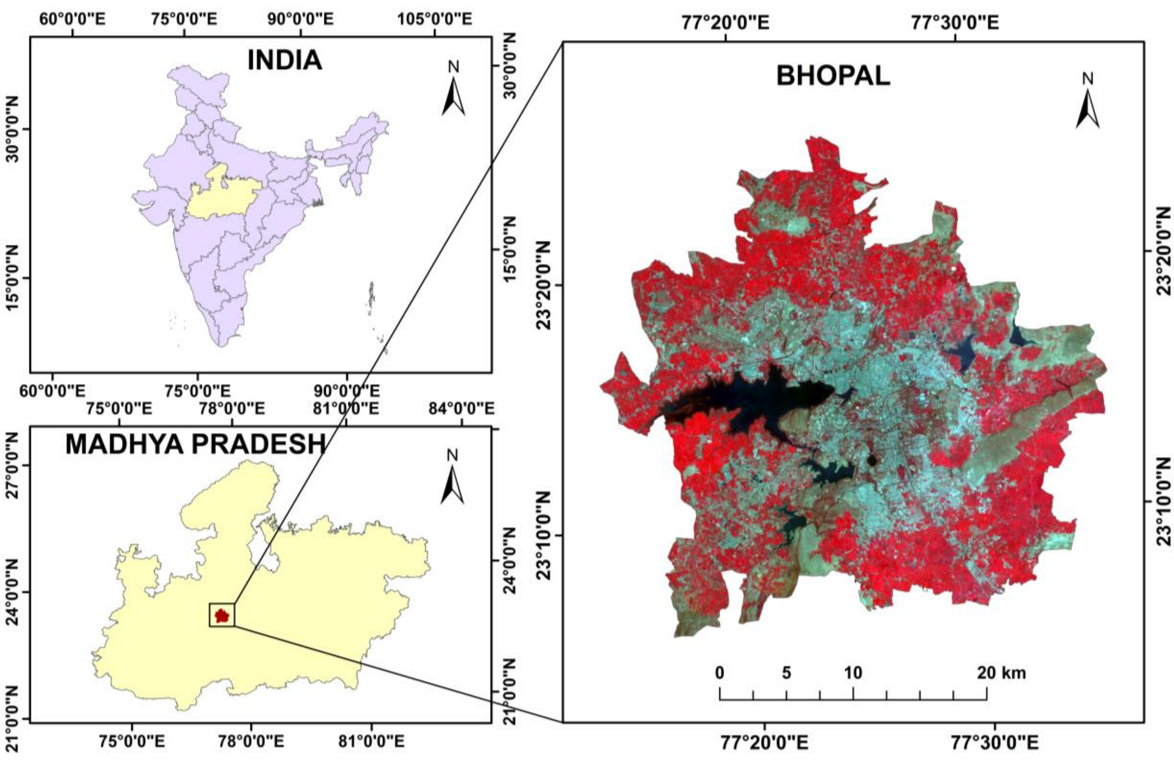

Figure 1. Study area map

Table 1. Datasets used

Data	Satellite/Sensor	Resolution	DOA	Remarks
LULC	Landsat8/OLI	30m	24 Feb 2022	Row/Path (145/044)
	Landsat8/OLI	30m	18 Feb 2014	
NTL	NPP/VIIRS	500m	Annual average	NOAA/VIIRS/DNB/MONTHLY_V 1/VCMSLCFG

Night-time light (NTL): NPP/VIIRS (Suomi National Polar-orbiting Partnership/Visible Infrared Imaging Radiometer Suite) data is used for night-time lights study. NPP/VIIRS is available after 2013, hence we selected the year 2014 and 2022 for our investigation. VIIRS data used here is Stray Light Corrected Night-time Day/Night Band Composites Version 1. This product uses a method to account for stray light and is an alternative configuration of the VIIRS DNB. This product excludes data impacted by cloud cover. The imagery of VIIRS night-time light offers night-time grid-based radiance values (nanoWatts/sr/cm^2).

4. METHODOLOGY

In this investigation, NTL data is utilised as major urbanity metrics. Land cover data is also utilised to extract the urban areas and calculate urban densities. An association between the results generated by both these methods is established. The study is conducted for an eight-year interval (2014-2022). The objective of this research is to: (a) Delineate the built-up land and estimate urban sprawl in each time-step using satellite image classification and NTL data, (b) Evaluate the change in urban built-up area and urban densities with respect to the change in NTL of the area.

The flowchart of the methodology adopted is shown in Fig. 2.

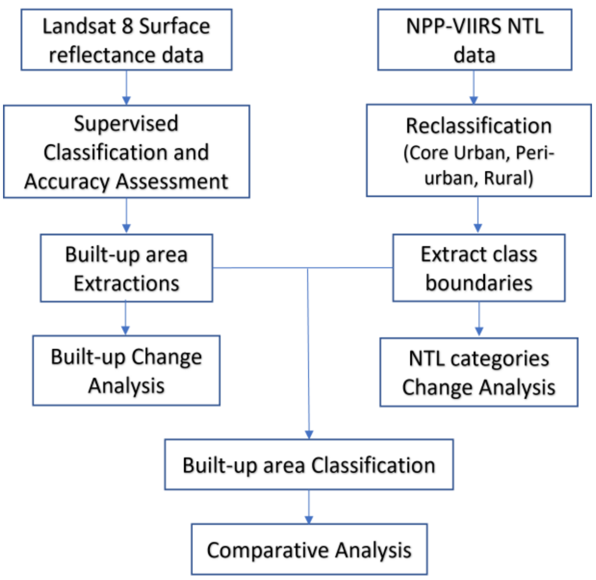

Figure 2. Methodology

Supervised Classification of Landsat images

Firstly, Landsat 8 images are classified for obtaining the LULC for the years 2014 and 2022. For reference, Google Earth images are employed since they enable inferences about land uses, such as detached buildings, commercial spaces, etc., that are not achievable with Landsat data alone. The classification is done to obtain four classes: (1) Built-up land, (2) Waterbody, (3) Vegetation, and (4) Bare land. Built-up land comprises of buildings, roads, pavements and parking areas, and all open areas with man-made surfaces. Vegetation class includes all trees, plants, agricultural lands, and grasslands. Water bodies cover all big and small lakes and ponds. Bare land comprises of rocks, hilly terrain with no vegetation and non-agricultural empty lands. For this, the power of Google Earth Engine (GEE), a cloud-based computing platform, is utilised. The supervised classification technique employing the machine learning algorithm Random Forest (RF) is used for LULC classification of Landsat images. It is found in the previous studies that RF is easy to use, requires less training time and give high classification and prediction accuracy (Lorena et al., 2011). The classified maps are then exported as Geotiff files for further processing in ArcGIS 10.3 and the regions depicting urban areas are extracted. Spatial change analysis of the extracted urban land is done from the year 2014 to 2022.

Secondly, accuracy assessment is done for overall accuracy and kappa coefficient in GEE again. A higher level of accuracy is often preferred for urban research because urban regions can have complex and varied land cover patterns. A Kappa value of 0.70 or higher and an overall accuracy of 85% or better is often considered as acceptable standards for LULC (Arumugam, Yadav, & Kinattinkara, 2021; Rwanga & Ndambuki, 2017).

Thirdly, the images are reclassified to just 2 classes, namely, ‘Urban’ and ‘Others’. The ‘Others’ class comprises all non-urban classes, i.e., water bodies, vegetation and bare land. The area occupied by the Urban class and change experienced by it in the 8-year study period is calculated.

Finally, the urban density per square kilometre is calculated. In order to analyze built-up density, we employed a grid-based approach. A grid of 1km x 1km cells was overlaid on the urban regions of both 2014 and 2022. By doing so, we divided the built-up areas into uniform square sections. To calculate the built-up density per square kilometer, we determined the area of built-up land within each 1km x 1km cell in both 2014 and 2022. This grid-based approach facilitated a spatially explicit analysis of built-up density patterns, enabling us to identify areas of high population concentration and assess the rate and magnitude of urban growth within specific regions.

Classification using Night-time Light images

In our study, we utilized night light images obtained at a resolution of 1 km from the Google Earth Engine (GEE) platform. These images provide annual average values of night time illumination for the study area. To analyze these images and categorize the complete study area, we employed three classification methods using ArcGIS 10.3. The first method, called "Manual," involved the user defining the cell values to determine the class intervals. The second method, "Natural breaks," and the third method, "Equal interval," automatically assigned cell range values based on the inherent characteristics of the data. The categorization techniques and the corresponding cell range values used in each method are presented in Table 2. The "Natural breaks" and "Equal interval" techniques relied on the system to assign appropriate cell ranges, while the "Manual" approach allowed user-defined intervals. This categorization helps in understanding the spatial patterns and intensity of night time illumination in the planning area of Bhopal, providing insights into urbanization and economic activity. The Natural Break method, which produces the most average outcomes out of the three reclassification techniques, is used in further research (Yücer & Erener, 2018).

Table 2. Pixel range values for NTL images categorisation using three approaches.

Year	Class	Natural break	Equal Interval	Manual
2014	1	0 - 7.1	0 - 15.7	0 – 12
	2	7.1 - 17.8	15.7 – 31.2	12 – 25
	3	17.8 - 46.7	31.2 – 46.7	25 – 46.7
2022	1	0 - 7.7	0 - 15.8	0 – 12
	2	7.7 - 18.4	15.8 – 31.1	12 – 25
	3	18.4 - 46.4	31.1 – 46.4	25 – 46.4

*The pixel range values are in nanoWatts/sr/cm^2

The pixels classified as class 1, 2, and 3 respectively represent the areas of low, medium and high luminosity during the night. This also depict the level of developments and economic activities in these areas, which is analogous to the level of luminosity. These images are then reclassified as 'Core urban', 'Peri-urban' and 'Rural' areas for the class numbers 3, 2, and 1 respectively, following the criteria as shown in Table 2. Secondly, the number of pixels lying in each of these classes is found out for 2014 and 2022. The change and percentage change in these values is computed for a better analysis.

Relationship between reclassified LULC maps and reclassified NTL images

The boundaries of the three classes of NTL images, are used to categorise the extracted built-up area into similar three classes as NTL images. The average built-up density (area of built-up land in km^2 per km^2) in each of these three classes is calculated and compared with each other. Change results of built-up land area and average built-up density were evaluated with respect to the NTL data to understand how change in urban sprawl has affected the artificial light radiance.

5. RESULTS AND DISCUSSIONS

Supervised LULC Classification Analysis

The findings from our study indicate that the overall classification accuracies for the years 2014 and 2022 were 85.38% and 84.12% respectively (Table 3), demonstrating a reliable performance of the classification method. The corresponding kappa values of 0.73 and 0.72 also indicate substantial agreement between the classified maps and the reference data. Furthermore, our analysis revealed that the total built-up area in 2014 was measured to be 63.60 km^2. By 2022, this built-up area had expanded to 91.10 km^2 (Table 4), indicating an increase of 27.50 km^2. This increment represents a significant growth rate of approximately 43% compared to the initial built-up area in 2014. In other words, the built-up area expanded at a rate of more than 5% annually over the studied period. This is due to the densification of the urban population, which in turn caused tremendous amount of growth in the urban night-time lights during the study period indicating an increase in both the population and economic activity in the city.

Table 3. Classification accuracy

Accuracy	2014	2022
Kappa	0.73	0.72
Overall	85.38%	84.12%

Table 4. Change analysis of built-up land

Class	2014	2022	Change	% Change
Built-up	63.60	91.10	27.50	43%

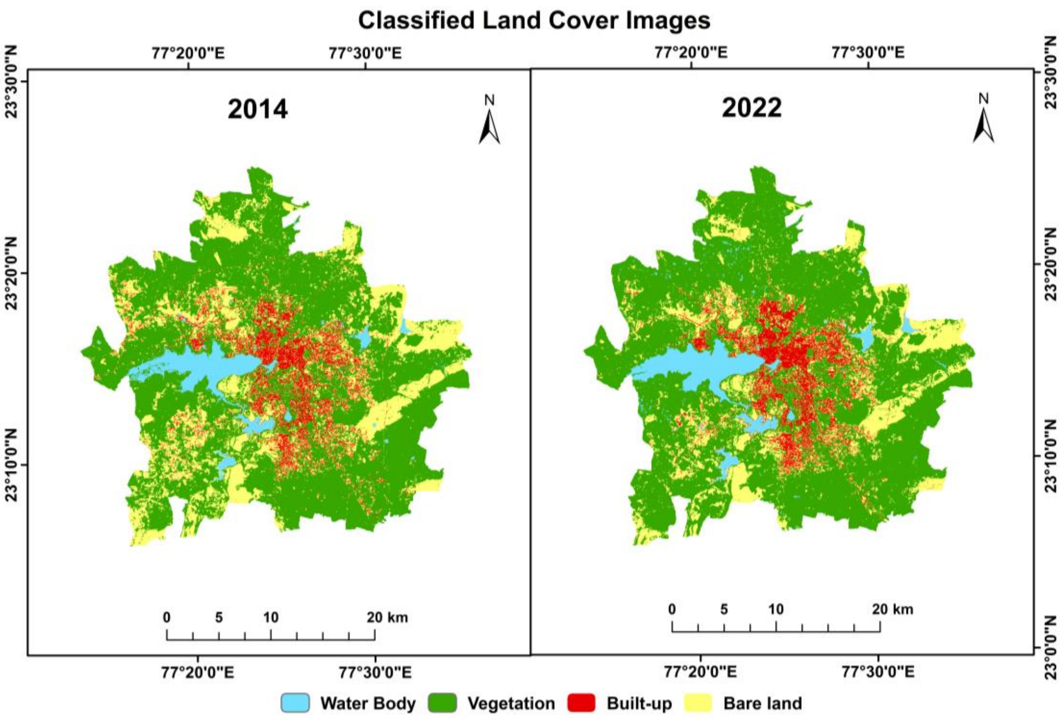

Figure 3. Classified maps representing Land Cover for 2014 and 2022

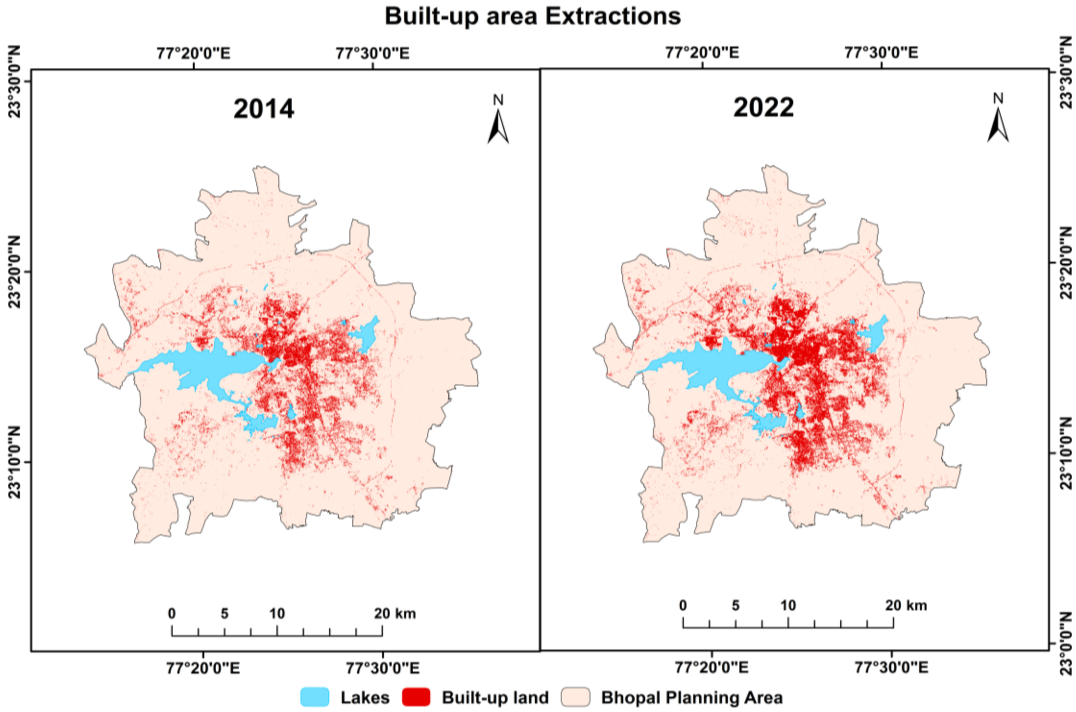

Figure 4. Built-up area extraction maps of 2014 and 2022

Figure 3 displays the classified maps representing the study area for the years under investigation. These maps were generated as a result of the LULC classification process applied to the study area in GEE. The classified maps visually depict the distribution and spatial patterns of different LULC classes within the study area for each specific year. Figure 4 represents the built-up area extractions for the same years. By comparing the classified maps, and built-up extractions across different years, changes in different classes can be visually observed, highlighting the dynamics of urbanization.

Night-time Lights Analysis

Figure 5 depicts the night time lights of Bhopal during the study period, covering the entire study area. The visual comparison of the two images provides clear evidence of an increase in the number of pixels with higher levels of luminosity. This increment is observed throughout the study area, with particularly pronounced higher relative values concentrated towards the city centre. These findings suggest significant economic activities taking place in the city, which justifies the observed changes in urbanization.

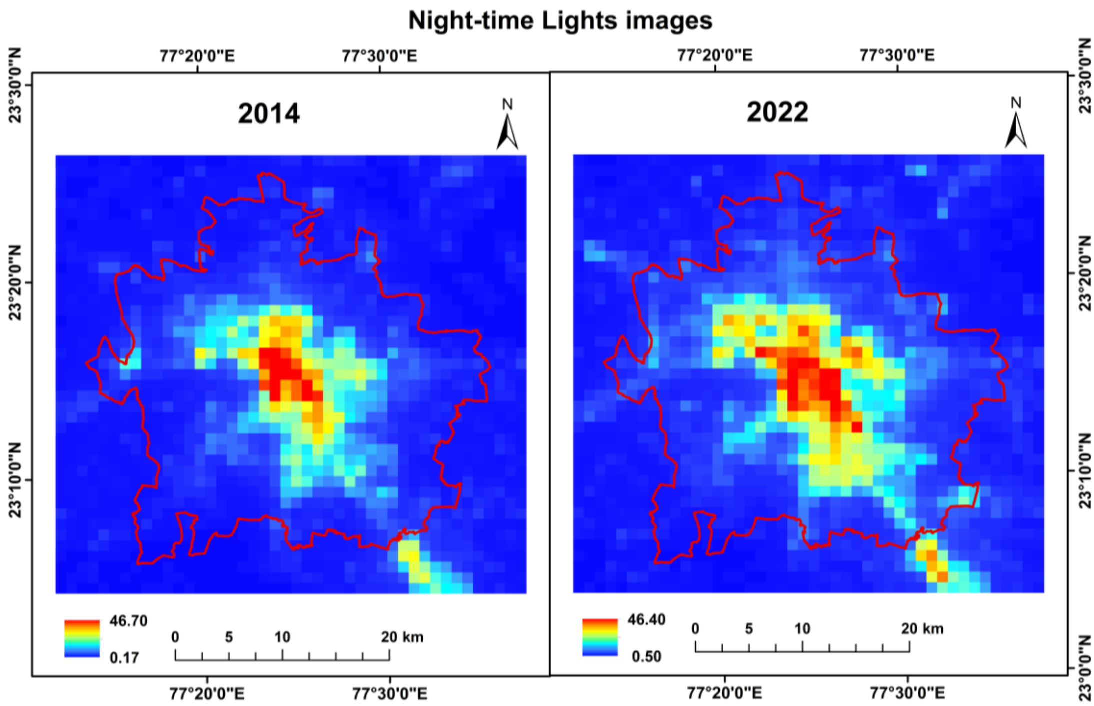

Figure 5. Night-time lights

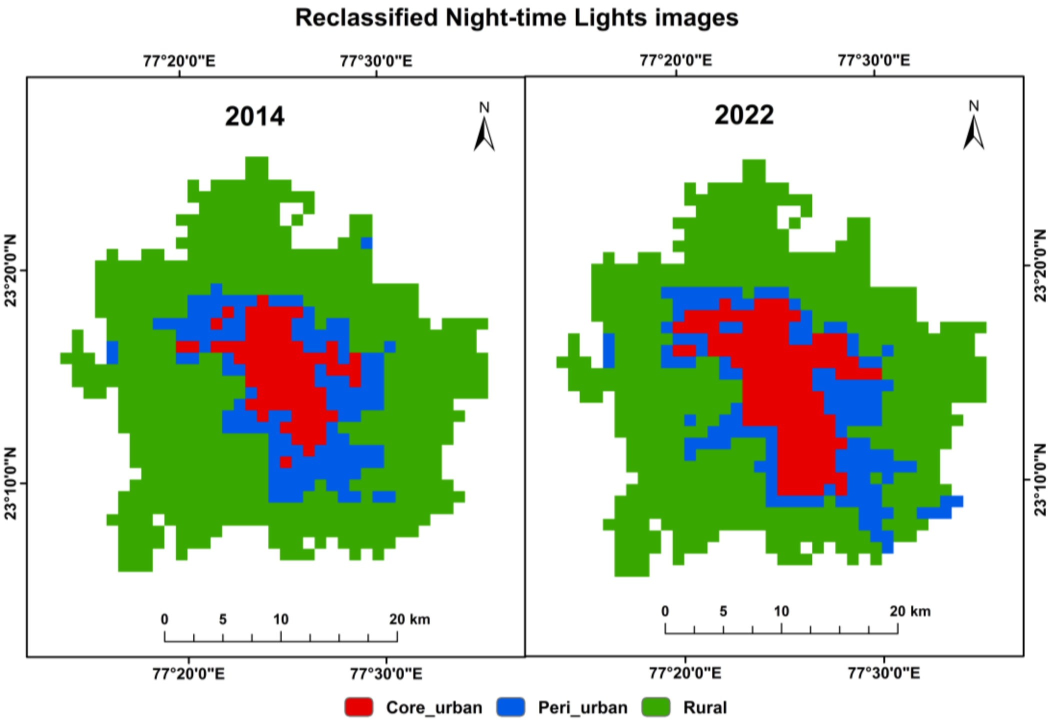

Figure 6. Night-time lights Reclassified images of 2014 and 2022

Table 5. Change number of pixels in different class of NTL

Class	2014		2022		Change	% Change	Remark
	Pixels (P_a)	%	Pixels (P_b)	%	(P_a -P_b)	(P_a -P_b)/ P_a	
Core Urban	80	9.8	127	15.5	47	58.75	Increase
Peri Urban	129	15.8	135	16.5	6	4.6	Increase
Rural	608	74.4	555	68	-53	-8.7	Decrease

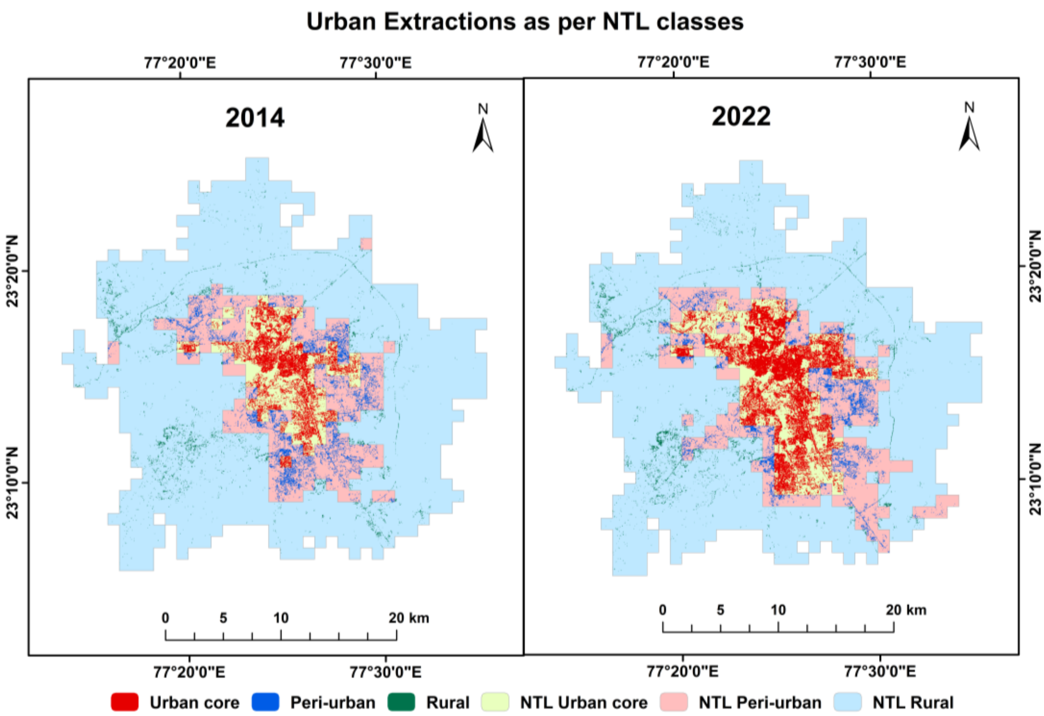

Figure 7. Urban Extractions as per the NTL classification

Table 6. Built-up area (km^2) in different NTL classes

Year	Core Urban	Peri-urban	Rural
2014	31.64	22.11	9.85
2022	61.45	19.35	10.3

Table 7. Average built-up density in different NTL classes

Year	Core Urban	Peri-urban	Rural
2014	0.385	0.173	0.023
2022	0.398	0.089	0.017

*The values are in km^2 of built-up land per km^2

Further analysis that was carried out, was done by categorising the NTL data into 3 classes using the criteria as shown in Table 2. All three methods of reclassification were applied, and upon evaluation, it was determined that the 'natural breaks' method provided the most optimal categorization. The post-classification results are depicted in Figure 6.

Post-classification, the number of pixels of the NTL image falling under each of these three categories for both the years is recorded. Change in number of pixels falling in each of these classes and the percentage change is computed as shown in Table 5. The proportion of 'core urban' pixels experienced substantial growth, increasing from 9.8% to 15.5% of the total number of pixels between 2014 and 2022. This represents a notable increase of 58.75%. Conversely, the 'peri-urban' pixels saw a smaller increase of 4.6%, while the 'rural' pixels witnessed a decline of 8.7% in the total study area. These changes can be attributed to the progressive conversion of 'rural' pixels into 'peri-urban' areas, and subsequently, the transformation of 'peri-urban' areas into 'core urban' regions.

By utilizing the boundaries of the respective three NTL categories, we classified the built-up area for the years 2014 and 2022. Subsequently, we calculated the total built-up area within each of these categories, as detailed in Table 6. The findings of this analysis are visually represented in Figure 7. Furthermore, we computed the average built-up density for different NTL classes, as outlined in Table 7. Notably, the average built-up density of the 'core urban' area exhibited an increase from 0.385 in 2014 to 0.398 in 2022. Conversely, there was a decline in the values for both the 'peri-urban' and 'rural' areas. This trend can be attributed to the gradual conversion of 'rural' pixels into 'peri-urban' areas and 'peri-urban' areas transforming into 'core urban' regions.

6. CONCLUSION

The results of the research emphasize the significance of remote sensing data in monitoring spatial and temporal changes in an area. This data enables researchers to analyze land use and land cover changes, urban expansion, and other environmental factors. The results of the study provide valuable insights into the dynamics of urbanization, highlighting the extent of urban growth and the need for effective urban planning and management strategies to accommodate the expanding urban areas. It also indicates high economic activities undergoing in the city which justifies the change in urbanisation and gentrification patterns occurring thereby. The analysis concluded that the urban expansion is triggered by huge influx of population from neighbouring areas because of increased economic activities in the city. It can also be concluded from the results that time series night light data enhances the ability to recognise urbanisation trajectories by evolving the urban characteristics as seen via a single pixel through time. Also, the more the urban activities dominate an area, higher is the chance that NTL data correctly identifies it as urbanised. A rising migration of residents from neighbouring towns as a result of new economic activity, such as a university and other services, businesses, led to the urban expansion of Bhopal.

The future research can be focussed on other aspects/attributes of the current study. Night-time lights data can be calibrated and validated using ground-truth data, such as building inventories, census information, or high-resolution imagery. By comparing the radiance values from satellite data with known physical attributes of buildings, statistical relationships can be established. Also, various modelling and machine learning techniques can be employed to establish a relationship between night-time lights data and built-up volume. It's important to note that while night-time lights data can provide a rough estimate of built-up volume and urbanization, it has limitations. Factors such as lighting efficiency, cultural or social practices, and the presence of natural features (e.g., lakes or forests) can influence the relationship between lights and built-up volume. Therefore, integrating night-time lights data with other datasets and employing appropriate validation techniques are crucial for accurate analysis.

REFERENCES

Arumugam, T., Yadav, R. L., & Kinattinkara, S. (2021). Assessment and predicting of LULC by Kappa Analysis and CA Markov model using RS and GIS Techniques in Udham Singh Nagar District, India. *Preprint*.

Cohen, B. (2006). Urbanization in developing countries: Current trends, future projections, and key challenges for sustainability. *Technology in Society*, *28*(1–2), 63–80. https://doi.org/10.1016/j.techsoc.2005.10.005

Government of MP. (2020). *Bhopal Development Plan-2031, Volume – I*. 150. Retrieved from http://mptownplan.gov.in/LU-panel/Bhopal/Amrut/ENGLISH/VOL1.pdf

He, X., Zhang, Z., & Yang, Z. (2021). Extraction of urban built-up area based on the fusion of night-time light data and point of interest data. *Royal Society Open Science*, *8*(8). https://doi.org/10.1098/RSOS.210838

Kabanda, T. H. (2022). Using land cover, population, and night light data to assess urban expansion in Kimberley, South Africa. *South African Geographical Journal*, *104*(4), 539–552. https://doi.org/10.1080/03736245.2022.2028667

Levin, N., & Duke, Y. (2012). High spatial resolution night-time light images for demographic and socio-economic studies. *Remote Sensing of Environment*, *119*, 1–10. https://doi.org/10.1016/j.rse.2011.12.005

Li, X., Li, D., Xu, H., & Wu, C. (2017). Intercalibration between DMSP/OLS and VIIRS night-time light images to evaluate city light dynamics of Syria's major human settlement during Syrian Civil War. *International Journal of Remote Sensing*, *38*(21), 5934–5951. https://doi.org/10.1080/01431161.2017.1331476

Liu, M., Liu, X., Zhang, B., Li, Y., Luo, T., & Liu, Q. (2022). Analysis of the evolution of urban nighttime light environment based on time series. *Sustainable Cities and Society*, *78*. https://doi.org/10.1016/J.SCS.2021.103660

Lorena, A. C., Jacintho, L. F. O., Siqueira, M. F., Giovanni, R. De, Lohmann, L. G., De Carvalho, A. C. P. L. F., & Yamamoto, M. (2011). Comparing machine learning classifiers in potential distribution modelling. *Expert Systems with Applications*, *38*(5), 5268–5275.

https://doi.org/10.1016/J.ESWA.2010.10.031

Ma, T., Zhou, Y., Zhou, C., Haynie, S., Pei, T., & Xu, T. (2015). Night-time light derived estimation of spatio-temporal characteristics of urbanization dynamics using DMSP/OLS satellite data. *Remote Sensing of Environment*, *158*, 453–464. https://doi.org/10.1016/J.RSE.2014.11.022

Massetti, L. (2020). Drivers of artificial light at night variability in urban, rural and remote areas. *Journal of Quantitative Spectroscopy and Radiative Transfer*, *255*. https://doi.org/10.1016/j.jqsrt.2020.107250

Rehman, S., Honap, V., Siddiqui, A., Maske, A., & Maithani, S. (2021). Spatio-Temporal Variations in Night Lights, Economy and Night Light Emissions in States of India. *Journal of the Indian Society of Remote Sensing*, *49*(12), 2933–2943. https://doi.org/10.1007/S12524-021-01427-1

Rwanga, S. S., & Ndambuki, J. M. (2017). Accuracy Assessment of Land Use/Land Cover Classification Using Remote Sensing and GIS. *International Journal of Geosciences*, *08*(04), 611–622. https://doi.org/10.4236/ijg.2017.84033

Seto, K. C., & Fragkias, M. (2005). Quantifying spatiotemporal patterns of urban land-use change in four cities of China with time series landscape metrics. *Landscape Ecology*, *20*(7), 871–888. https://doi.org/10.1007/S10980-005-5238-8/METRICS

Shukla, A., Jain, K., Ramsankaran, R. A. A. J., & Rajasekaran, E. (2021). Understanding the macro-micro dynamics of urban densification: A case study of different sized Indian cities. *Land Use Policy*, *107*(March), 105469. https://doi.org/10.1016/j.landusepol.2021.105469

Singh, S., & Jain, K. (2022). Geospatial Approach for Urban Environmental Quality Assessment. *International Archives of the Photogrammetry, Remote Sensing and Spatial Information Sciences - ISPRS Archives*, *43*(B3-2022), 705–711. https://doi.org/10.5194/isprs-archives-XLIII-B3-2022-705-2022

Wang, L., Fan, H., & Wang, Y. (2019). An estimation of housing vacancy rate using NPP-VIIRS night-time light data and OpenStreetMap data. *International Journal of Remote Sensing*, *40*(22), 8566–8588. https://doi.org/10.1080/01431161.2019.1615655

Weng, Q. (2012). Remote sensing of impervious surfaces in the urban areas: Requirements, methods, and trends. *Remote Sensing of Environment*, *117*, 34–49. https://doi.org/10.1016/J.RSE.2011.02.030

Yücer, E., & Erener, A. (2018). GIS Based Urban Area Spatiotemporal Change Evaluation Using Landsat and Night Time Temporal Satellite Data. *Journal of the Indian Society of Remote Sensing*, *46*(2), 263–273. https://doi.org/10.1007/s12524-017-0687-5

Zhang, Q., & Seto, K. C. (2013). Can night-time light data identify typologies of urbanization? A global assessment of successes and failures. *Remote Sensing*, *5*(7), 3476–3494. https://doi.org/10.3390/RS5073476